EUROPEAN ORGANIZATION FOR NUCLEAR RESEARCH
ORGANISATION EUROPEENNE POUR LA RECHERCHE NUCLEAIRE

CERN - PS DIVISION

PS/RF Note 2001-003
CERN-NUFACT-NOTE 062

REVISED BEAM DYNAMICS AND LAYOUT FOR THE SUPERCONDUCTING SECTION OF THE SPL[1)]

Frank Gerigk

ABSTRACT

Since the publication of the SPL conceptual design report [1] the beam dynamics and the layout of the linac were subject to several changes. As the studies of the room temperature part of the linac [2] show practically no emittance growth, the longitudinal emittance in the SC section of the SPL is reduced from 0.6 to 0.3 π deg MeV. This measure enhances the longitudinal debunching effect in the transfer line between the SPL and the Proton Driver Accumulator Compressor rings (PDAC). A modified layout for this transfer line which stretches the bunches in phase and compensates energy and phase jitter from the linac is presented. A new matching tool for the IMPACT code is used to improve the transitions between the different sections of the linac. Furthermore the results of a study concerned with cavity vibrations [3] is taken into account to readjust the synchronous phases in the linac. Finally a new alternative for the high energy section of the linac is tested, which uses no LEP cavities and which reduces the linac length by almost 90 m. The results of multiparticle simulations with matched and mismatched beams are presented for both versions.

Geneva, Switzerland
23 January 2001

[1)] Superconducting Proton Linac

1 Layout

One of the initial ideas, which motivated the SPL study was the recuperation of RF hardware from LEP after its shutdown. The assemblage of all available LEP cavities into a superconducting proton linac would yield an accelerating potential of approximately 3 GeV. However, the disadvantage of these cavities is that they are built for a particle velocity of $\beta = 1$ while in the SPL a maximum β of only 0.954 is reached at the output energy level of 2.2 GeV. To overcome the inefficiency of these cavities at even lower velocities, the SPL uses three additional types of cavities which are built for geometrical betas of 0.52, 0.7, and 0.8. The actual version of the SPL operates at 352 MHz and accelerates a pulsed beam of 18 mA bunch current up to the final energy of 2.2 GeV.

As the studies of the room temperature part of the linac ($\rightarrow$ 120 MeV) show practically no emittance growth [2], the longitudinal emittance of the SC section is now adapted to these results, i.e. it is reduced by 50% to 0.3 π deg MeV. This measure raises the space charge forces and slightly enhances the debunching process in the transfer line to the PDAC rings. Furthermore several changes were made in order to optimize the beam dynamics layout: Tückmantel [3] investigated the effect of cavity vibrations on the longitudinal stability of the beam. As a result of this study the average phase for the $\beta = 0.8$ section had to be decreased. It now starts with -20^o and is then gradually reduced down to -15^o towards the end of the section (former values: -15^o / -10^o, see [4]).

Between the $\beta = 0.7$ and $\beta = 0.8$ sections the acceleration per focusing period changes substantially. The periods become longer and the accelerating field almost doubles from 5 MeV to 9 MeV. In order to ease the matching between these two sections the gradient of the first eight cavities of the $\beta = 0.8$ section is slowly raised to the nominal level. Due to the lower average phase and the reduced gradient, one cryostat with LEP cavities was exchanged against one with $\beta = 0.8$ cavities. By this measure the output energy of the SPL could be kept above 2.2 GeV without lengthening the linac.

From 1100 MeV onwards the longitudinal phase advance becomes very low. Therefore it is possible to double the length of the focusing periods and to use two cryostats instead of only one between two quadrupole doublets. This measure reduces the number of quadrupole doublets by 25[1)] and shortens the linac by 8 m, what altogether reduces the costs by $\approx$ 3 MCHF.

Looking at the effective gradient[2)] of the four different types of cavities versus energy (Fig. 1) one can see that the LEP cavities always work less efficiently than the newly developed $\beta = 0.8$ cavities. On the one hand this is caused by the higher accelerating gradient: 9 MeV for $\beta = 0.8$, 7.5 MeV for the LEP cavities, but the main reason for the lower efficiency of the LEP cavities is the low transit time factor. At the transition between $\beta = 0.8$ and $\beta = 1$ the transit time factor of the $\beta = 0.8$ cavities is $\approx$ 40% higher, while only towards the end of the linac both transit time factors approach a common value. That means that even applying the latest surface treatment techniques in order to raise the gradient of the LEP cavities would not make them as efficient as the $\beta = 0.8$ cavities. Therefore the idea is tempting to replace the LEP cavities of the actual scenario by the new $\beta = 0.8$ cavities, and to see how this alternative compares with the previous one in terms of cost and performance. Table 1 summarizes the layout parameters of these two alternatives and Table 2 lists the main differences.

The difference in cost is mainly determined by the number and type of RF cavities, the number of magnets, the length of the tunnel, the cryogenic system, and the vacuum system. Figure 2 shows the relative change of cost, calculated from the SPL cost coefficients, for the high energy part of the linac when the transition energy between the $\beta = 0.8$ and $\beta = 1$ sections is shifted from the original value of 1.1 GeV towards the final energy of 2.2 GeV. The estimate does not include a change of the cryogenic transfer lines, the electricity network, the control system, and the instrumentation. It does also not include an already proposed [1] optimization of the

[1)] 13 in the linac and another 12 in the transfer line where the same focusing period is kept, see section 3 about modified transfer line.

[2)] 'Real estate' gradient including the length of the cut-off tubes

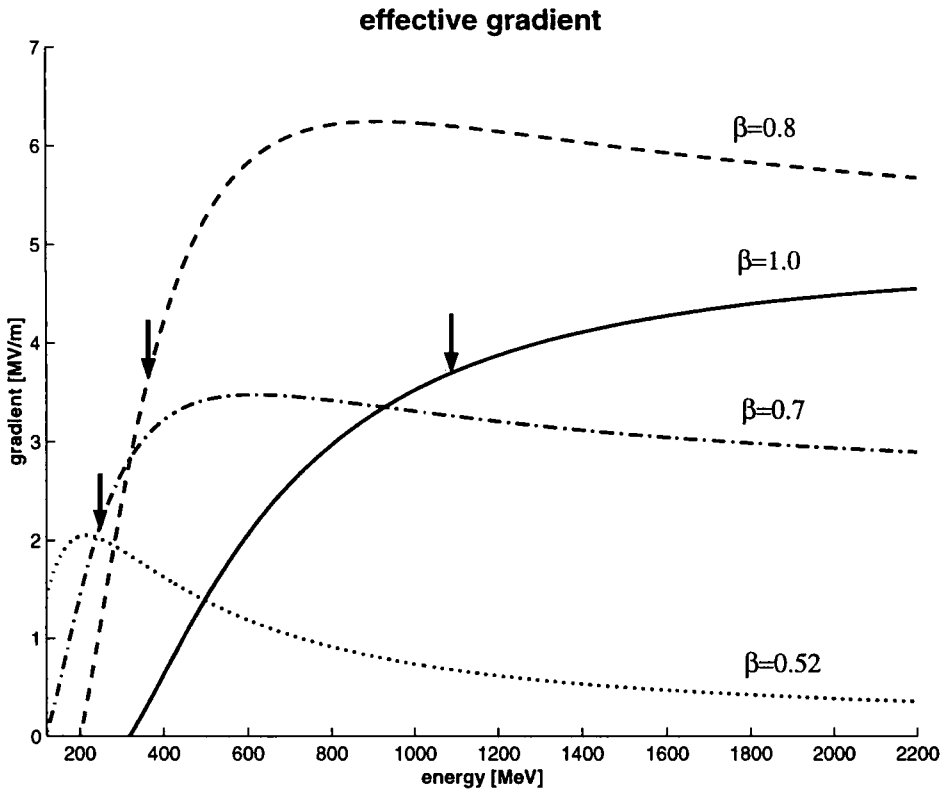

Figure 1: Effective gradients for the four sections / transition energies

Table 1: Layout parameters of SPL IIa (with LEP cavities) and SPL IIb (without LEP cavities)

section	β	$W_{in} \rightarrow W_{out}$ [MeV]	gradient [MV/m]	No. of cavities	No. of cryostats	No. of foc. per.	No. of ampl.*	$\phi_{av.}$ [deg]	length [m]
1	0.52	120 → 236	3.5	42	14	14	42 t	-25	101
2	0.7	236 → 383	5	32	8	8	32 t	-20	80
3	0.8	383 → 1111	9	52	13	13	13 k	-20/-15	166
4a	1.0	1111 → 2204	7.5	104	26	13	18-20 k**	-17	324
4b	0.8	1111 → 2235	9	76	19	9.5	19 k	-15	237

* two types of amplifiers: t - tetrodes, k - klystrons

** 18 klystrons for 4/6 cavities/klystron, 20 klystrons for 4/8 cavities/klystron

Table 2: Layout comparison of SPL IIa and SPL IIb

version	W_{out} [MeV]	N_{tot} cavities	N_{tot} cryostats	N_{tot} klystrons	length [m]
SPL IIa	2204	234	61	31-33**	671
SPL IIb	2235	202	54	32	584

cryogenic system for the $\beta = 0.8$ cavities. Apart from these uncertainties, one can see that the difference in cost between the two alternatives SPL IIa/b is about 4 MCHF, a small percentage of the total project costs.

The higher cost of the SPL IIb version is caused by the higher amount of required cooling power. The two cryoplants have to deliver 40 kW instead of 32 kW, a change that raises the capital costs of these facilities by $\approx$ 3.5 MCHF. Although the static losses go down with a lower number of cryostats, the dynamic losses of the $\beta = 0.8$ cavities are about 2.5 times higher, due to their higher gradient. A slightly lower gradient and an optimized temperature in the cryostats is likely

to reduce the necessary cooling power for these cavities.

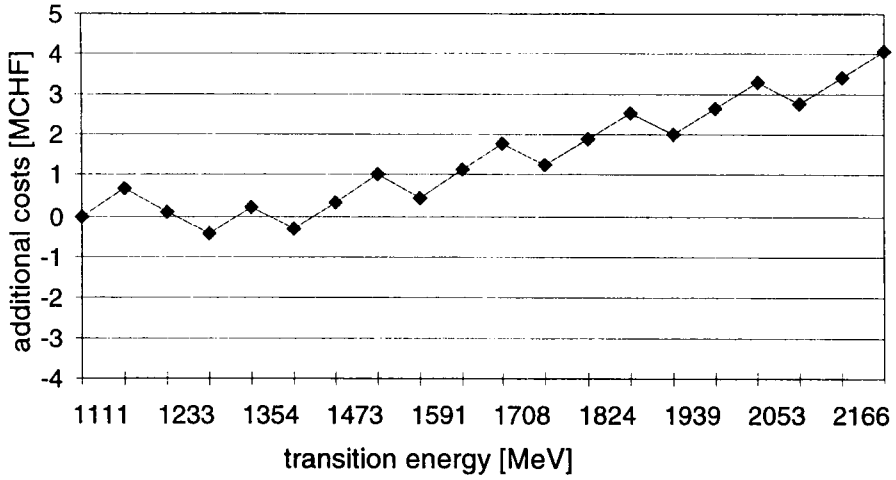

Figure 2: Additional costs for the high energy part of the SPL II for various transition energies between $\beta = 0.8$ and $\beta = 1.0$

2 Beam Dynamics

All multiparticle simulations were carried out with IMPACT [5], an object oriented parallel 3D particle-in-cell code. The beam dynamics layout, i.e. basically the choice of phase advances and average phases was designed with the help of the envelope code FIX3D [6]. The code was modified so that it automatically computes a matched envelope for every focusing period of the linac, and then provides the phase advance data for the matched solutions. In order to find a matched transition between different sections of the linac R.D. Ryne embedded FIX3D in MARYLIE [7], so that the fitting capabilities of MARYLIE can be used to vary beam line elements. The advantage of this approach is that now all codes use the same RF gap model, they all use the exact on-axis field distribution from SUPERFISH [8] and correctly treat the phase slippage in the multicell cavities.
The simulations were carried out with 1 million particles and a bunch current of 40 mA, which is more than twice the design current of the machine. The initial distribution is a 6D waterbag.

2.1 Design Principles

One of the guidelines for a smooth transition between two sections is to keep the phase advance per meter as smooth as possible. In Figure 3 one can see that although there are considerable jumps in the phase advance per period, the phase advance per meter is almost flat at the transition areas. At the transition between the $\beta = 0.7$ and the $\beta = 0.8$ section one can see the advantage of the slowly rising gradient in the first $\beta = 0.8$ cavities: instead of an abrupt jump to a higher phase advance per meter the curve rises slowly until the nominal accelerating gradient is reached. Apart from that the lattice is designed in such a way that the zero current phase advance is always kept well below 90^o. The curves for the SPL IIb are not printed here since they are almost identical to the SPL IIa curves in Figure 3.
In [9] and [10] it is shown that integer tune ratios σ_z/σ_x can yield emittance exchange induced by "collective resonances" and thereby excite beam instabilities. The actual SPL II design avoids crossing these areas by careful adjustment of the transverse focusing lattice (see Fig. 4). Despite the relatively modest tune depression along the SPL II (≈ 0.7 in all three planes for energies below 1 GeV, Fig. 4) emittance exchange could be observed, when crossing the areas of integer tune ratios. Since emittance exchange becomes more significant for strongly nonequipartitioned beams, another guideline for the presented design is to keep the nonequipartitioning factor[3)] as

[3)] here defined as longitudinal over transverse beam temperature

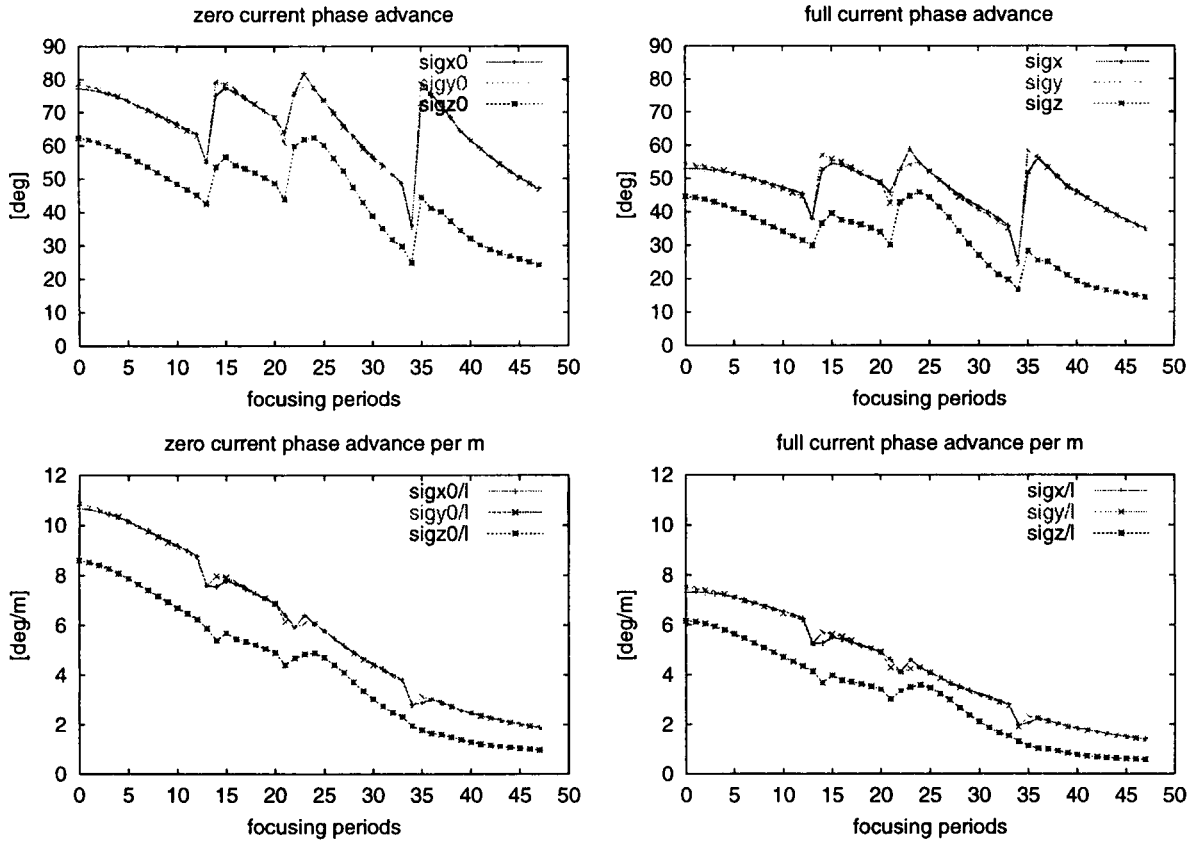

Figure 3: Phase advance curves for the SPL IIa

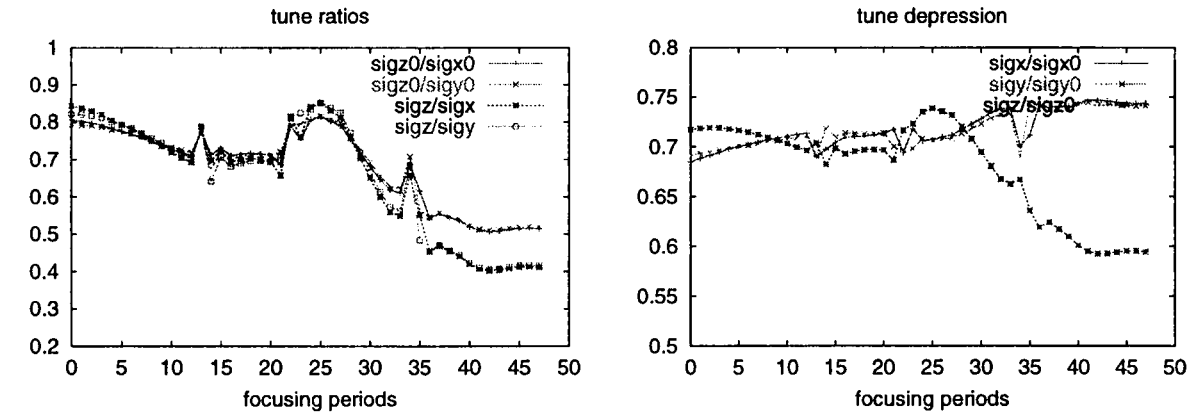

Figure 4: Tune ratio and tune depression for SPL IIa

low as possible (Fig. 5). A detailed study of the above mentioned principles will be presented in a seperate paper.

2.2 Simulation Results

Both versions of the linac show a smooth evolution of the beam radii (Fig. 6). Neither emittance growth nor development of beam halo can be observed for the nominal case. Due to the longer focusing periods above 1.1 GeV, the transverse beam radius in the last section is bigger than for the previous layout (SPL I) but there is still a factor of 30 between the r.m.s. beam radius and the beam pipe radius.

Figure 7 shows that the maximum phase slip of the SPL IIb at the linac end is almost three times bigger than for the SPL IIa. Nevertheless, no filamentation or halo development could be

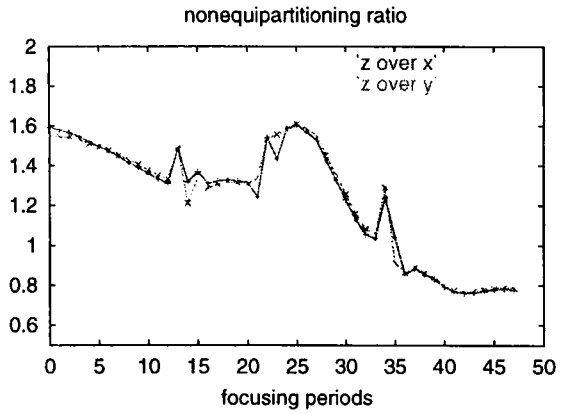

Figure 5: Nonequipartitioning factor (longitudinal over transverse temperature) for SPL IIa

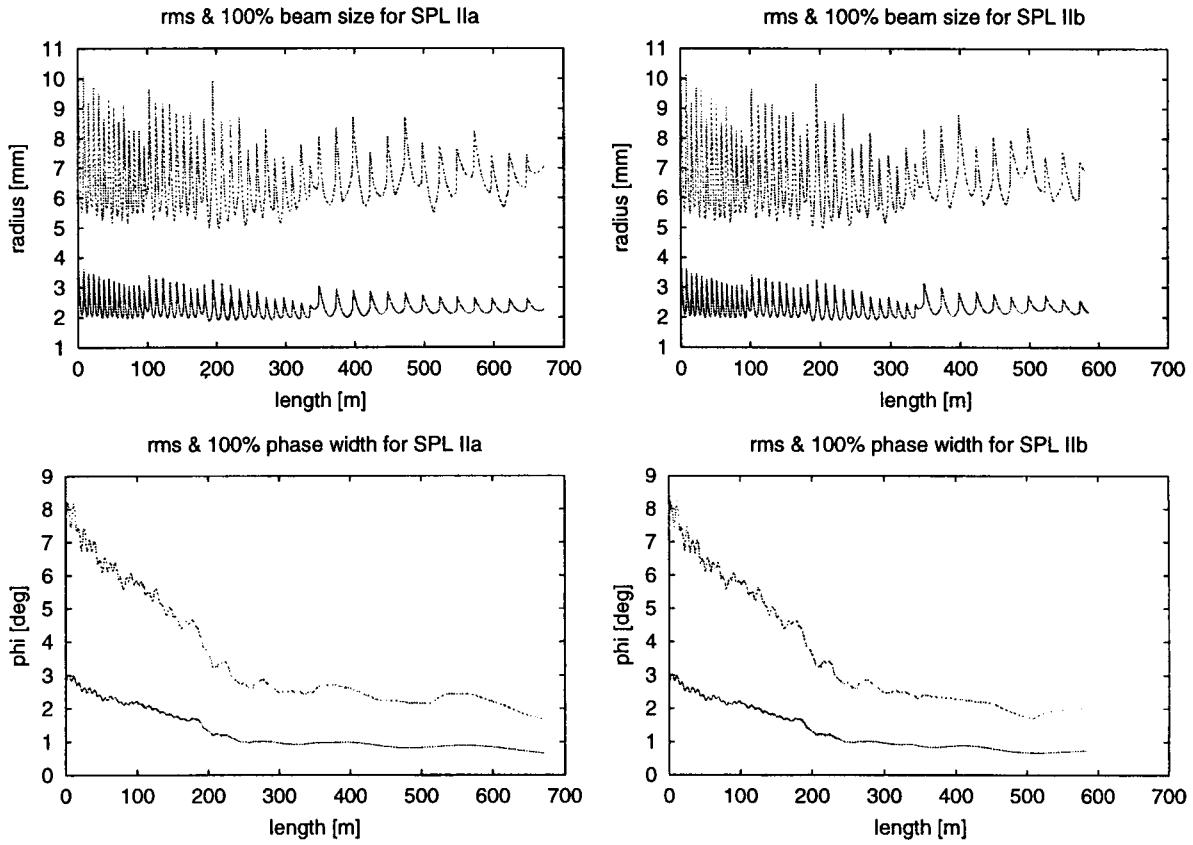

Figure 6: Evolution of beam radii for SPL IIa (left) and SPL IIb (right)

observed. Even in the mismatched cases the two layouts showed no particular difference in the output distributions.

The stability of the design against errors is studied with three different mismatched input beams:

1. +30% radial mismatch in x and -30% in y, this corresponds to the excitation of the quadrupolar mode,
2. +30% radial mismatch in all three planes, a mixed excitation of transverse and longitudinal instabilities, and
3. +30% radial mismatch in the transverse planes and -30% in the longitudinal plane.

The initial mismatch is introduced at the beginning of the first quadrupole doublet. Figure 8 shows the emittance evolution for both linac versions with mismatched input beams.

One can see that also in the mismatched cases the results for the two layouts are almost exactly

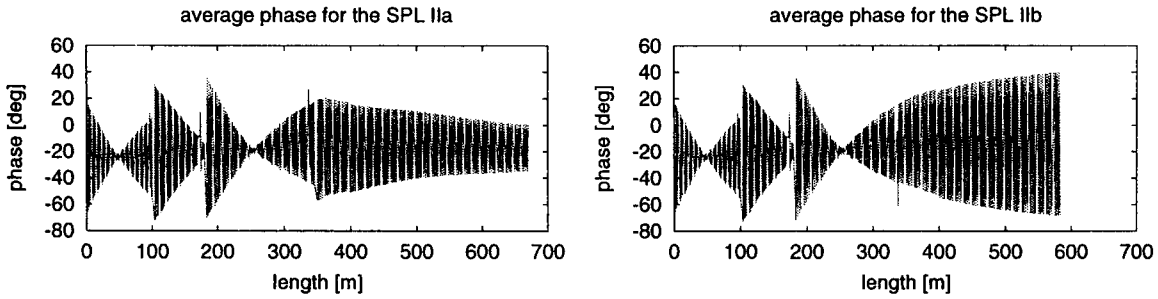

Figure 7: Phase slip for SPL IIa (left) and SPL IIb (right)

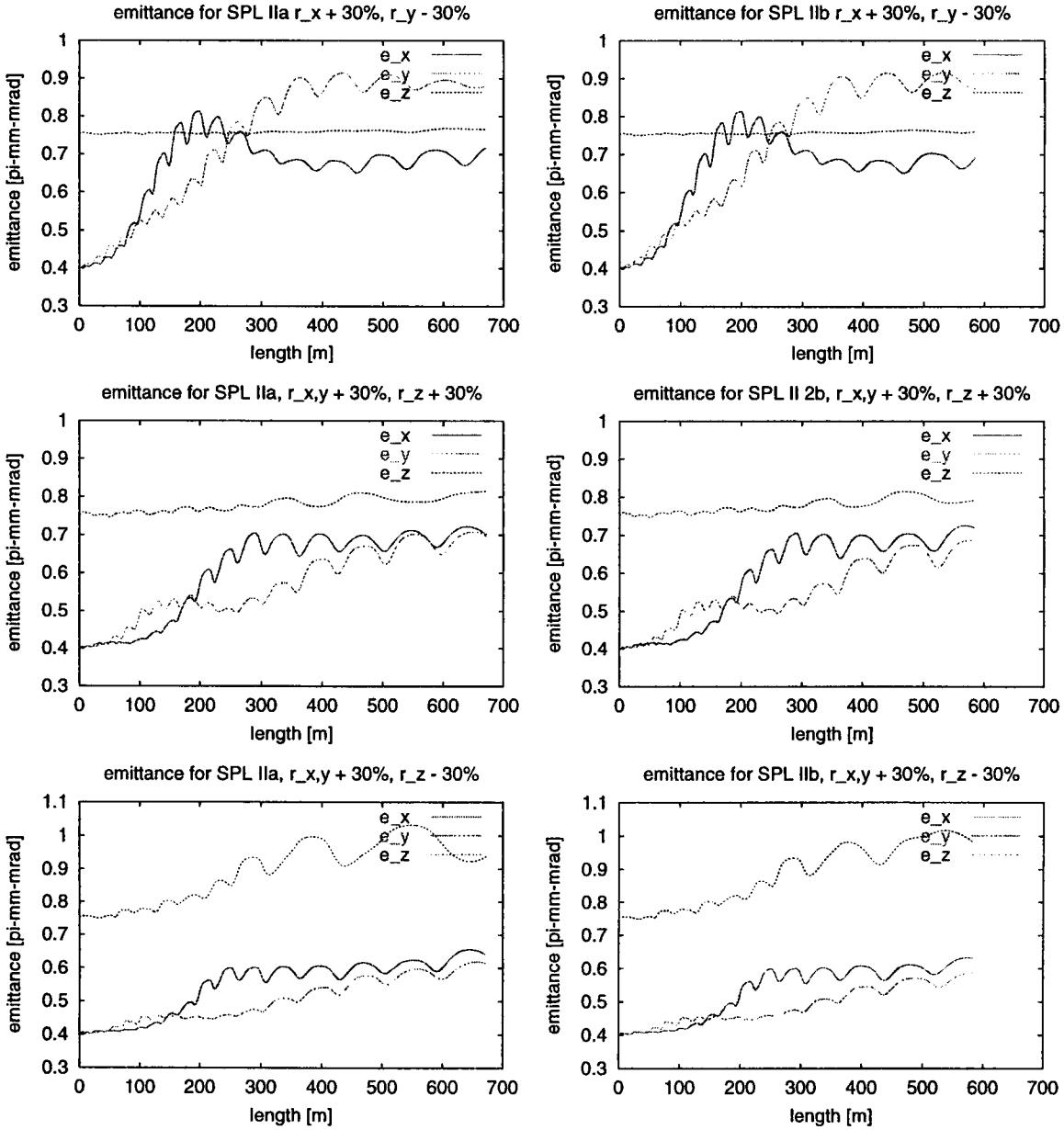

Figure 8: Emittance evolution for mismatched beams, SPL IIa (left) and SPL IIb (right)

the same, i.e. from the beam dynamics point of view there is no disadvantage in using the $\beta = 0.8$ cavities up to the end of the linac. Due to the low longitudinal phase advance in the high energy part of the linac, the beam is "stiff" enough as not to be disturbed by a big phase slippage.
The maximum transverse beam radius in the error cases never exceeds 20 mm, so that it appears reasonable to reduce the aperture radius of the quadrupole doublets from 100 to 60 mm. Figure 9 shows the beam size evolution for the third error case, were the disturbance of the beam envelope oscillations was found to be most distinct. Nevertheless, no uncontrolled blow up of the beam can be observed, neither transversely nor longitudinally. Please note that all the results presented here are simulated with twice the nominal current, which means that the space charge forces are doubled compared to the design case. The emittance growth rates for 18 mA bunch current are almost half as big.

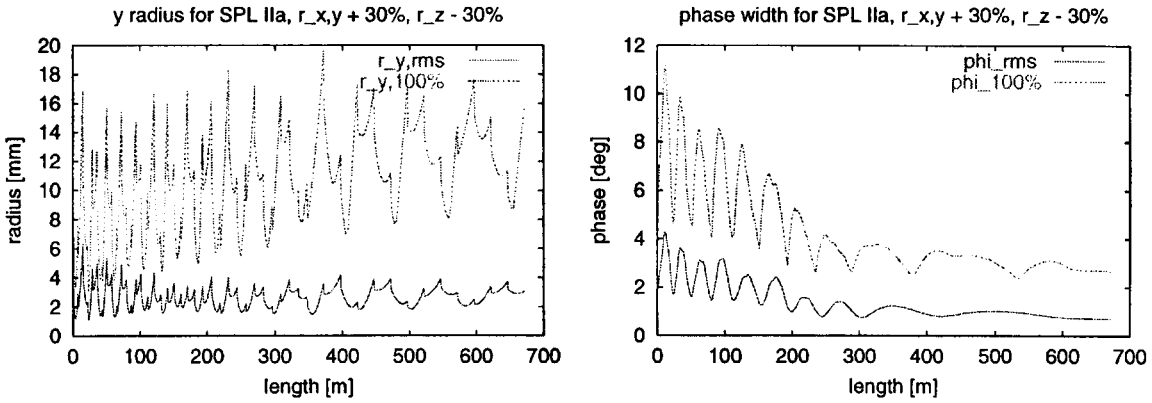

Figure 9: Beam size evolution for the SPL IIa, $r_{x,y} + 30\%$, $r_z - 30\%$

Finally Figure 10 shows the phase space plots for the worst cases. Since the difference between the two linac version is again negligible only the plots for the SPL IIa are given.

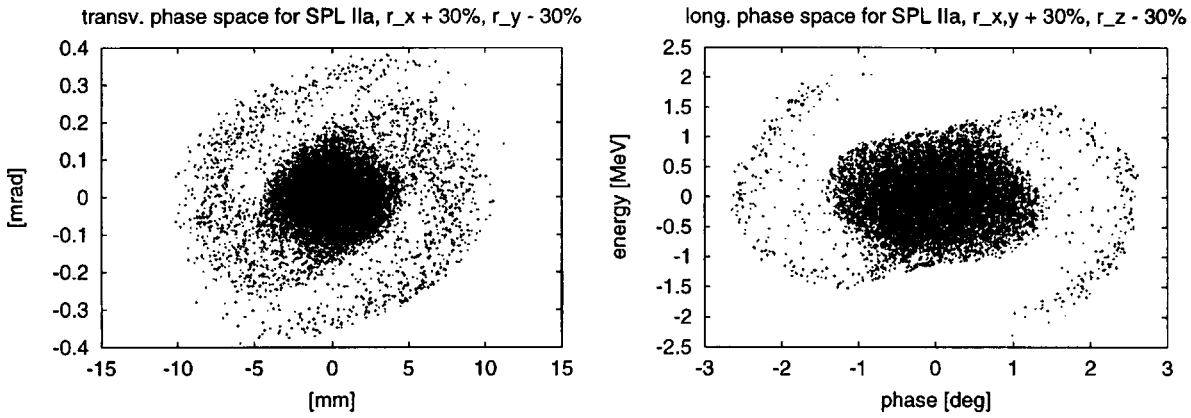

Figure 10: Phase space plots for the SPL IIa, left: y-py for $r_x + 30\%$, $r_y - 30\%$, right: z-pz for $r_{x,y} + 30\%$, $r_z - 30\%$

3 Transfer line to the Accummulator Compressor Rings

The transfer line consists of four debunching cavities, a drift, and a final bunch rotator. Its task is to stretch the bunches in phase and to compress their energy width. At the same time the transfer line is used as "jitter compressor" which reduces the energy and phase jitter from the linac. A detailed description of the design of such a line is given in [11].
Due to the smaller longitudinal emittance the debunching process during the drift is slightly faster than in the previous linac design. For the new layout (Table 3) the resulting total bunch

length is set to 16^o at 352.2 MHz corresponding to 130 ps. Compared to the reference secenario in [11] the new transfer line is shortened from 256 m to 200 m and the number of quadrupoles is reduced from 20 to 8. The acceptance for energy and phase jitter from the linac remains almost the same: $\pm 9^o$ or ± 9 MeV for single offsets, and about $\pm 5.5^o$ / ± 5.5 MeV for simultaneous phase and energy offsets. Matched beams with the quoted offsets are transformed such that they fit into the $\pm$ 2 MeV RF bucket of the accumulator compressor rings. The simulations of the transfer line were made without taking into account the effect of bending dipoles. The evolution of matched and mismatched linac bunches through the rings is under study and it is likely that the layout of the line is subject to further changes.

Table 3: Parameters for the modified transfer line

element	length [m]	no. of cavities	no. of focusing periods	cavity voltage [MV/m]	average phase [deg]
debuncher	12.8	4	0.5	7.5	$+90^o$
drift	175.2		7		
buncher	11.7	4	0.5	3.1	-90^o
total	199.7	8	8		

4 Conclusions

A lower synchronous phase for the $\beta = 0.8$ and $\beta = 1.0$ was chosen to increase the stability against cavity vibrations. With the help of a new matching tool the transitions between the different sections of the linac were improved. It was found that a smooth phase advance per meter in the transition areas eases the matching and raises the stability against errors. Matching between sections is done by variation of existing beam line elements in the transition area.
It was shown that a 50% lower longitudinal emittance (0.3 π^o MeV instead of 0.6) is feasible and does not affect the stability of the system.
The length of the focusing periods above 1.1 GeV was doubled in order to increase the low longitudinal phase advance per period. By this measure also the transverse phase advance could be increased without driving the beam into a highly nonequipartitioned state. Furthermore the new layout saves 25 quadrupole doublets and some meters of tunnel.
The transfer line to the accumulator and compressor rings was adapted to the new focusing periods and the lower longitudinal emittance.
An alternative layout for the high energy part of the linac was tested, which uses $\beta = 0.8$ cavities up to the end of the linac. The results of the multiparticle simulations show an almost equal beam evolution for both versions. This also means that it is possible to shift the transition energy between $\beta = 0.8$ and LEP cavities to any suitable value without affecting the output beam. The new layout shortens the tunnel by $\approx$ 90 m, while only slightly increasing the costs. However, the reduced number of cavity types in the linac might be an operational advantage, and a more precise cost analysis should be made when the parameters of the cryogenic system will be better known. Also the partitioning of four cavities per klystron eases the vector sum control of the cavity parameters, when compared to the six cavities per klystron scheme that applies for the SPL version with LEP cavities. Another advantage of skipping the LEP cavities is that the linac design no longer suffers from the 100 Hz mechanical resonance of the LEP cavities. This opens up the possibility of pulsing the machine at 50 Hz (now 75 Hz) and of coupling the pulse frequency to the mains. Since all the other cavity types are still under development, it should be possible to design them such that their mechanical resonances are no integer multiples of 50 Hz. Furthermore a pulse frequency of 50 Hz reduces the RF power in the normalconducting part of the linac as well as in the nc 44/88 MHz cooling channel of the actual neutrino factory scenario. Both versions were tested with three different strongly mismatched beams and with twice the design current. In no case were particles lost on the outer wall. The maximum transverse beam radius is well kept within 20 mm, which means that the aperture radius of the quadrupoles can

be set to 60 mm (formerly 100 mm) without risking particle loss. Although the longitudinal emittance is 50% lower than in the previous version (SPL I, see [1]), the r.m.s. emittance growth in the error case could be kept in the same range. In the transverse plane a maximum emittance growth of 110% (formerly 100%) was observed, and the worst longitudinal case showed an emittance growth of 30% (formerly 50%).

Table 4: Simulation results for the SPL IIa and SPL IIb for 40 mA bunch current

	in	out	mismatch out*	unit
$\varepsilon_{x,y,r.m.s.,norm}$	0.4	0.41	0.88	[π-mm-mrad]
$\varepsilon_{z,r.m.s.,norm}$	0.3	0.3	0.37 (0.39)	[π^o-MeV]
$r_{x,y,r.m.s.}$	3.6	2.6	3.7	[mm]
$r_{x,y,100\%}$	10	7.5	17 (16)	[mm]
$\Delta E_{r.m.s}$	0.1	0.48 (0.41)	0.53 (0.58)	[MeV]
$\Delta E_{100\%}$	0.3	1.55 (1.2)	2.6 (2.0)	[MeV]
$\Delta\phi_{r.m.s.}$	2.8	0.65 (0.73)	0.73 (0.78)	[°]
$\Delta\phi_{100\%}$	7.8	1.7 (2.0)	2.7 (3.0)	[°]

*for the worst case

Table 5: General parameters for the SPL IIa and SPL IIb

Particles	H^-
Kinetic energy	2.2 GeV
RF frequency	352.2 MHz
Mean beam power	4 MW
Nominal pulse current	11 mA
Nominal bunch current	18.4 mA
Simulated bunch current	40 mA
Repetition rate	75 Hz

References

[1] Ed: M. Vretenar. Conceptual Design of the SPL, a High-Power Superconducting H- Linac at CERN. CERN 2000-012 Yellow Report, 12/2000.

[2] F. Gerigk; M. Vretenar. Design of the 120 MeV Drift Tube Linac for the SPL. CERN-NUFACT-NOTE 37, CERN, Geneva, 2001.

[3] J. Tückmantel. Simulation of the SPL SC RF System with Beam using SPLinac. SL-Note-2000-054, CERN, Geneva, 2000.

[4] F. Gerigk. Beam Dynamics in the Superconducting Section of the SPL (120MeV - 2.2GeV). CERN-NUFACT-NOTE 24, CERN, Geneva, 2000.

[5] J. Qiang; R.D. Ryne; S. Habib; V. Decyk. An Object-Oriented Parallel Particle-In-Cell Code for Beam Dynamics Simulation in Linear Accelerators. Journal of Computational Physics 163, pp. 1-18, 2000.

[6] R.D. Ryne. Finding matched rms envelopes in rf linacs: A Hamiltionian approach. LANL, Los Alamos, NM 87545, 1995.

[7] A.J. Dragt. *MARYLIE 3.0 User's Manual, A Program for Charged Particle Beam Transport Based on Lie Algebraic Methods.* Center for Theoretical Physics, University of Maryland, 2/1999.

[8] J.H. Billen; L.M. Young. *Poisson, Superfish - Documentation LA-UR-96-1834.* LANL, 1999.

[9] I. Hofmann. Stability of anisotropic beams with space charge. In *Physical Review E 57, 4713*, 1998.

[10] J-M. Lagniel; S. Nath. On Energy Equipartition Induced by Space Charge in Bunched Beams. In *Proceedings of EPAC 98, 1118*, 1998.